Journal of Magnetism and Magnetic Materials 415 (2016) 82–86

Contents lists available at ScienceDirect

Journal of Magnetism and Magnetic Materials

journal homepage: www.elsevier.com/locate/jmmm

Magneto-optical switching of Bloch surface waves in magnetophotonic crystals

M.N. Romodina, I.V. Soboleva [1], A.A. Fedyanin *

Faculty of Physics, Lomonosov Moscow State University, Moscow 119991, Russia

ARTICLE INFO

Article history:
Received 6 September 2015
Received in revised form
20 November 2015
Accepted 12 January 2016
Available online 21 January 2016

Keywords:
Bloch surface electromagnetic wave
Magnetophotonic switching
Magnetophotonic crystals
Magneto-optical Faraday rotation

ABSTRACT

Bloch-surface-wave (BSW) excitation controlled by Faraday rotation in one-dimensional magnetophotonic crystals is presented. Dispersion curves of the Bloch surface wave and waveguide modes of magnetophotonic crystals consisting of silicon dioxide and bismuth-substituted yttrium-iron-garnet (Bi:YIG) quarter-wavelength-thick layers are calculated using Berreman's 4×4 transfer matrix method. Enhanced Faraday rotation observed in the magnetophotonic crystals in the spectral vicinity of the BSW resonance enables the magneto-optical switching of BSWs. The excitation of the BSWs at the magnetophotonic crystal surface for *p*-polarized incident light is induced by magneto-optical activity in the Bi:YIG layers.

1. Introduction

Bloch surface waves (BSWs) propagating in all-dielectric photonic crystals [1,2] can be considered as a dielectric analogue of surface plasmons with fewer losses. Due to their high quality factor, BSWs are mainly applied for sensing [3–6]. Recently, BSWs have been considered as appropriate for 2D optical systems required in optoelectronic components and optical integrated devices [7]. 2D elements, including lenses and waveguides, have been proposed to manipulate the BSW surface propagation [8,9]. The control of the BSW excitation and propagation using external variable factors is essential and worth consideration.

The proper polarization state of the incoming light is crucial for BSW generation; thus, external magnetic field represents promising candidate for controlling BSWs using magneto-optical Faraday rotation. One-dimensional photonic crystals with magnetic activity, namely magnetophotonic crystals (MPCs), consisting of alternating layers of magnetic and non-magnetic materials [10,11] support BSW propagation [12] and, at the same time, provide the appreciable value of the Faraday rotation angle [13–15]. The appearance of the allowed modes in the MPC photonic band gap leads to light localization and further enhancement of magneto-optical [16–18] and nonlinear magneto-optical effects [19,20]. Recently, MPCs have been shown to support the generation of optical Tamm states at the interface between MPC and uniform media with negative permittivity, for example, a metal or a non-magnetic photonic crystal. The Faraday rotation has been shown to be enhanced in the vicinity of Tamm state resonance [21,22]. The magneto-optical manipulation of optical Tamm states has been suggested [23] but requires specially designed structures [24]. The sensitivity of the BSW to the polarization of incident light represents the simplest way of realizing control of the BSW excitation and propagation in MPCs by the external magnetic field.

In this paper, magneto-optical switching of the BSW in the MPC controlled with an external magnetic field is studied using Berreman's 4×4 transfer matrix approach. The reflectance and the corresponding Faraday rotation spectra are numerically studied in the vicinity of the BSW resonance.

2. Methods

Berreman's 4×4 matrix method [25–28] is used for the MPC optical and magneto-optical response calculations. The Kretschmann configuration of the attenuated total internal reflection scheme is supposed to be used for the BSW excitation (Fig. 1). We consider the propagation of a plane electromagnetic wave with a frequency ω and wave vector k that is incident from a glass prism on the one-dimensional MPC back surface. An elementary cell of the MPC consists of one non-magnetic and one magneto-active $\lambda/4$-layer. The directions of the coordinate axes are shown in Fig. 1.

The equation for the tangential components of the electric and magnetic field of the plane wave is determined from Maxwell's equations and can be written as follows:

* Corresponding author.
E-mail address: fedyanin@nanolab.phys.msu.ru (A.A. Fedyanin).
[1] *Also at*: Frumkin Institute of Physical Chemistry and Electrochemistry, Russian Academy of Sciences, Moscow 119071, Russia.

http://dx.doi.org/10.1016/j.jmmm.2016.01.034
0304-8853/

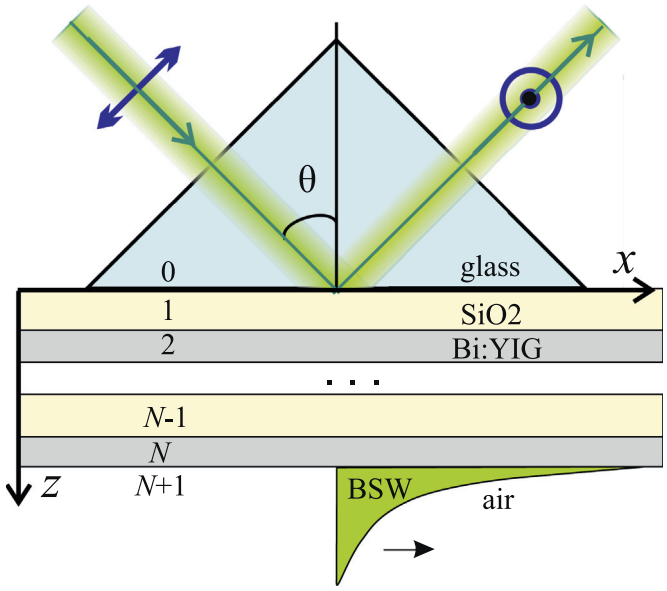

Fig. 1. Schematic of the BSW excitation at the surface of the MPC in the Kretschmann configuration.

$$\frac{\partial}{\partial z}\psi = \frac{i\omega}{c}\mathbf{\Delta}\psi, \tag{1}$$

where $\psi = \{E_x, H_y, E_y, -H_x\}$ is a Berreman vector. The matrix $\mathbf{\Delta}$ has the following form for a magneto-active medium [25]:

$$\hat{\mathbf{\Delta}} = \begin{pmatrix} 0 & 1 - X^2/\varepsilon & 0 & 0 \\ \varepsilon & 0 & -ig & 0 \\ 0 & 0 & 0 & 1 \\ ig & 0 & \varepsilon - X^2 & 0 \end{pmatrix}, \tag{2}$$

where $X = k_x c/\omega$ depends on the angle of the plane wave incidence, ε is the electric permittivity of the medium, and g describes the magnetization-induced gyration of the material with magnetization along the z-axis. The matrix $\mathbf{\Delta}$ is constant along the z-axis in a homogeneous layer; thus, four eigenvalues q_j and four eigenvectors Ψ_j can be found for Eq. (1). In a magneto-optically active material, q_1 and q_2 correspond to a wave with left circular polarization propagating down and up, respectively, and q_3 and q_4 correspond to a wave with right circular polarization going down and up, respectively. If both $g \neq 0$ and $X \neq 0$, the eigenvalues have the following form:

$$q_{1,2} = \pm\frac{\omega}{c}\sqrt{\varepsilon - X^2 + \frac{g}{\varepsilon}\sqrt{\varepsilon(\varepsilon - X^2)}},$$
$$q_{3,4} = \pm\frac{\omega}{c}\sqrt{\varepsilon - X^2 - \frac{g}{\varepsilon}\sqrt{\varepsilon(\varepsilon - X^2)}}. \tag{3}$$

The propagation of the light wave from one side of a layer with thickness h to another side can be described as $\psi(z + h) = \mathbf{P}(h)\psi(z)$, where $\mathbf{P}$ takes the form

$$\mathbf{P}(h) = \mathbf{\Psi}\mathbf{K}\mathbf{\Psi}^{-1}. \tag{4}$$

At this point, we can find the propagation matrix $\mathbf{K}(h)$ to account for the phase and amplitude changes in the field vector components going from the top to the bottom side of the layer. $\mathbf{K}$ is a diagonal matrix with elements:

$$K_{jj} = \exp[iq_j h]. \tag{5}$$

The matrix $\mathbf{\Psi}$ relates the field vector components in the layer to the tangential electric and magnetic field at the boundary of the layer and consists of the four eigenvectors Ψ_j of Eq. (1). For magneto-optically active media, $\mathbf{\Psi}$ has the following components:

$$\mathbf{\Psi} = \begin{pmatrix} 1 & 1 & 1 & 1 \\ cq_1/\omega & cq_2/\omega & cq_3/\omega & cq_4/\omega \\ \frac{i\sqrt{\varepsilon - X^2}}{\sqrt{\varepsilon}} & \frac{i\sqrt{\varepsilon - X^2}}{\sqrt{\varepsilon}} & -\frac{i\sqrt{\varepsilon - X^2}}{\sqrt{\varepsilon}} & -\frac{i\sqrt{\varepsilon - X^2}}{\sqrt{\varepsilon}} \\ \frac{iq_1 c\sqrt{\varepsilon}}{\omega\sqrt{\varepsilon - X^2}} & \frac{iq_2 c\sqrt{\varepsilon}}{\omega\sqrt{\varepsilon - X^2}} & -\frac{iq_3 c\sqrt{\varepsilon}}{\omega\sqrt{\varepsilon - X^2}} & -\frac{iq_4 c\sqrt{\varepsilon}}{\omega\sqrt{\varepsilon - X^2}} \end{pmatrix}. \tag{6}$$

For a non-magnetic layer, the matrices $\mathbf{P}$ can be found analogously by assuming $g=0$ in Eq. (2).

We use the s–p polarization basis to calculate the reflectance of the plane wave and Faraday rotation of its polarization plane. In this basis, a plane wave in layer n is described by the vector $\mathrm{E}_n = (E_p^+, E_p^-, E_s^+, E_s^-)$ consisting of four mode amplitudes propagating in the layer, where p and s correspond to p- and s-polarizations of light and $+$ and $-$ correspond to propagation up and down. At the top edge of layer n, Berreman's vector ψ can be converted to E_n as [26]

$$\psi = \mathbf{\Pi}_n \mathrm{E}_n, \tag{7}$$

and the matrix $\mathbf{\Pi}_n$ in the non-magnetic isotropic dielectric layer takes the following form:

$$\mathbf{\Pi}_n = \begin{pmatrix} \sqrt{\varepsilon_n - X^2}/\sqrt{\varepsilon_n} & \sqrt{\varepsilon_n - X^2}/\sqrt{\varepsilon_n} & 0 & 0 \\ \sqrt{\varepsilon_n} & -\sqrt{\varepsilon_n} & 0 & 0 \\ 0 & 0 & 1 & 1 \\ 0 & 0 & \sqrt{\varepsilon_n - X^2} & -\sqrt{\varepsilon_n - X^2} \end{pmatrix}. \tag{8}$$

Finally, the optical properties of a magneto-optical structure consisting of N layers are determined by the transfer matrix $\mathbf{T}$ connecting the field vectors of plane waves that are incident, reflected and transmitted through the structure [26]:

$$\mathbf{T} = \mathbf{\Pi}_{N+1}^{-1}\mathbf{P}_N\mathbf{P}_{N-1}\mathbf{P}_{N-2}\ldots\mathbf{P}_2\mathbf{P}_1\mathbf{\Pi}_0, \tag{9}$$

where $\mathbf{\Pi}_0$ describes the entrance media, namely, the glass prism, and $\mathbf{\Pi}_{N+1}$ relates to the output media, namely, air. Denote $r_{i,j}$ as the amplitude reflectance coefficients for an incident wave in mode j into mode i, where i and j correspond to the number of components of the vector E. These amplitude reflectance coefficients can be obtained using elements of the transfer matrix $\boldsymbol{T}$ [26]:

$$r_{2,1} = (T_{24}T_{41} - T_{21}T_{44})/D,$$
$$r_{4,1} = (T_{21}T_{42} - T_{22}T_{41})/D,$$
$$r_{2,3} = (T_{24}T_{43} - T_{23}T_{44})/D,$$
$$r_{4,3} = (T_{23}T_{42} - T_{22}T_{43})/D, \tag{10}$$

where $D = (T_{22}T_{44} - T_{24}T_{42})$. The intensity reflectance R and Faraday rotation angle F can be calculated as

$$R = \left(r_{2,1}^2 + r_{4,1}^2\right)E_1^2 + \left(r_{2,3}^2 + r_{4,3}^2\right)E_3^2;$$
$$F = \arctan\left(\frac{r_{2,1}E_1 + r_{2,3}E_3}{r_{4,1}E_1 + r_{4,3}E_3}\right) - \arctan\left(\frac{E_1}{E_3}\right). \tag{11}$$

3. Results and discussion

A one-dimensional MPC with silica (SiO_2) non-magnetic layers and bismuth-doped yttrium-iron-garnet (Bi:YIG) magneto-active layers are considered. The SiO_2 layers have a thickness of 150 nm, and the thickness of the Bi:YIG layers is 90 nm. Both layers are $\lambda/4$

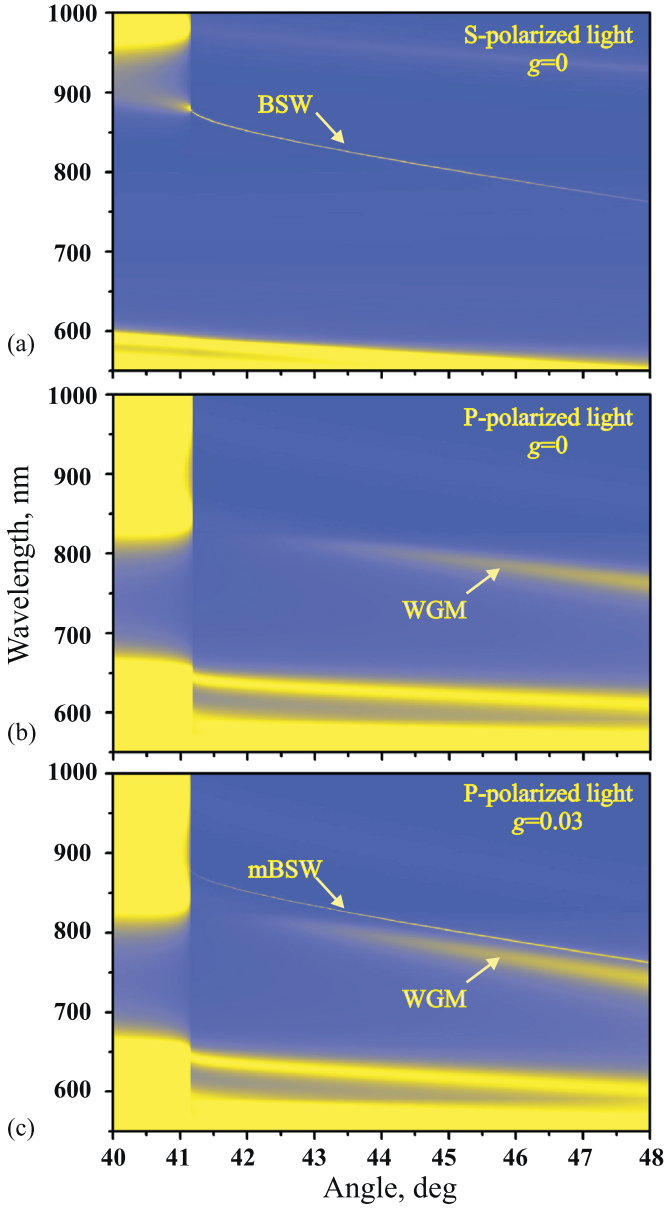

Fig. 2. Reflectance R versus angles of incidence θ and wavelength λ calculated for a 1D magnetophotonic crystal with 7 bilayers, where the thickness of the bottom layer is 28 nm. (a) — s-polarized light, magnetic field is absent, excitation of BSW, (b) — p-polarized light, magnetic field is absent, excitation of WGM. (c) — p-polarized light, magnetic field applied, g=0.03 for Bi:YIG layers, excitation of WGM and magnetic-field-induced BSW.

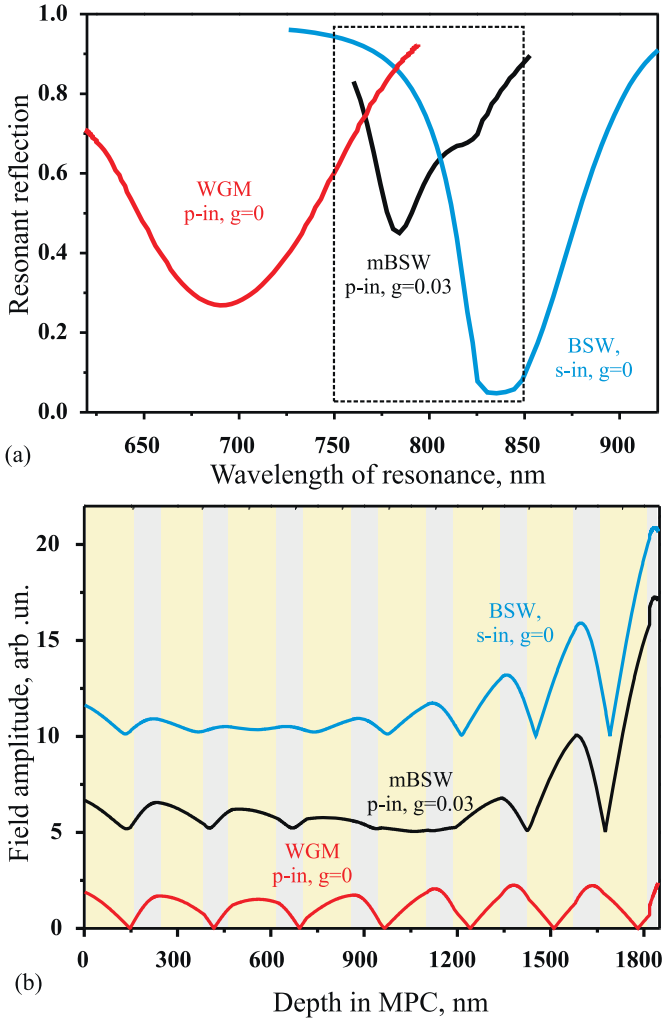

Fig. 3. (a) The reflectance at BSW, WGM and mBSW resonances as a function of the resonance wavelength, where the curves are obtained by varying the bottom layer thickness of the MPC containing 8 bilayers. (b) The BSW, WGM and mBSW field distribution inside the MPC at wavelengths of 792 nm, where the black and blue curves are shown with vertical shifts of 5 and 10 from zero, respectively. Angle of incidence equals 45°. Blue lines — s-polarized light, magnetic field is absent, resonance for BSW; red lines — p-polarized light, magnetic field is absent, resonance for WGM; black lines — p-polarized light, magnetic field applied, g=0.03 for Bi:YIG layers, resonance for mBSW. The region marked with a dashed frame in panel (a) is analysed in Fig. 5. (For interpretation of the references to colour in this figure caption, the reader is referred to the web version of this paper.)

for a wavelength of 870 nm, except for the bottom layer. The thickness of the bottom layer was varied to tune the wavelength of the BSW resonance. The numerical calculations were performed using the values of the real and imaginary components of the dielectric permittivity as a function of the light wavelength taken from [29] for SiO_2 and from [30] for Bi:YIG. The refractive index of the glass prism is 1.52, and the gyration g is taken as 0.03, which correlated to g values in Bi:YIG.

The MPC reflectance R versus angle of incidence θ and wavelength λ are shown in Fig. 2, where the angle of total internal reflection equals 41°. When no magnetic field is applied to the structure, if the incident light is s-polarized, the BSW is excited, and a narrow dip appears in $R(\lambda, \theta)$ at wavelengths from 750 to 870 nm and at angles from 41° to 48° (Fig. 2(a)). If the incident light has a p-polarization, $R(\lambda, \theta)$ exhibits a wide dip at lower wavelengths as a result of the excitation of the waveguided mode (WGM) inside the MPC and does not demonstrate the BSW excitation (see Fig. 2(b)). When a magnetic field is applied and when the Bi:YIG layers exhibit magneto-optical activity (g=0.03), the narrow dip corresponding to the magnetic-field-induced BSW (mBSW) excitation appears in the angular reflectance spectra for p-polarized incident light (Fig. 2(c)). The position of the mBSW resonance in the spectra is identical to the position of the BSW resonance for the s-polarized light. However, for the s-polarized light, the reflectance minimum corresponding to the BSW excitation is deeper for smaller angles, and the mBSW dip is more distinct for larger angles when the mBSW is closer to the WGM resonance. This means that both resonances being inherent in the MPC, the BSW for the s-polarized light and the WGM for the p-polarized light, thereby influence the magneto-optical switching of the mBSW.

The spectral positions of the BSW and WGM resonances are sensitive to the thickness of the bottom layer of the MPC. The spectral dependences of the reflectance at the BSW, mBSW or

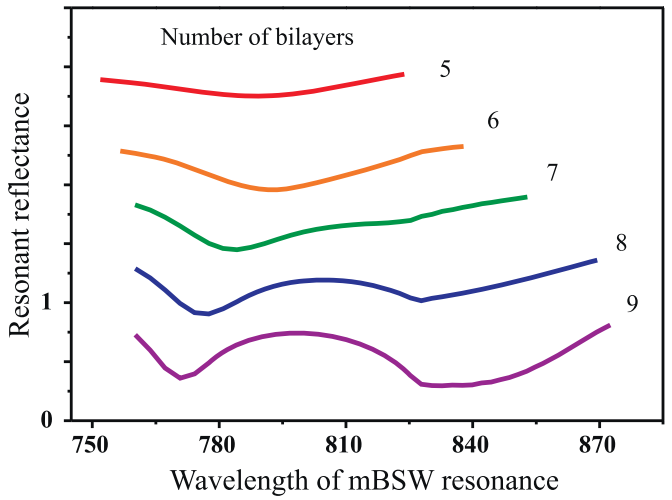

Fig. 4. The reflectance at the mBSW resonance as a function of resonant wavelength for different numbers of bilayers in the MPC. Curves are shown with vertical shifts equal to 0.5 relative to each other.

WGM resonance wavelength are shown in Fig. 3(a). The curves for the mBSW and BSW were obtained by varying the bottom layer thickness from 15 to 60 nm with a step of 0.5 nm. The curve for WGM was obtained by varying the bottom layer thickness from 5 to 200 nm with a step of 5 nm. The curve for the mBSW seems to be the superposition of the BSW and WGM curves. The field distributions of the BSW, mBSW and WGM inside the MPC are shown in Fig. 3(b). Both the BSW and mBSW exhibit high concentrations of electromagnetic fields near the MPC bottom surface and a 10-fold field enhancement compared to the incident plane wave.

Depending on the number of bilayers, the curve of the reflectance at the mBSW resonance as a function of resonance wavelength exhibits different shapes, as shown in Fig. 4. For small numbers of bilayers (approximately 5–6), the curve has one minimum at a wavelength of 790 nm. When the number of bilayers is greater than 6, the curve of reflectance at the mBSW exhibits two minima, corresponding to the resonance wavelengths of the WGM (lower wavelength) and the BSW (higher wavelength). The increase in the Q-factor with increasing MPC thickness makes both resonances of the BSW and WGM more pronounced, which leads to corresponding changes in the mBSW reflectance spectra.

The region of the mBSW resonance indicated by the dashed frame in Fig. 3(a) was studied in detail, and the MPC reflectance spectra were obtained with (Fig. 5(b)) and without a magnetic field (Fig. 5(a)) applied to the structure. When the bottom layer thickness equals 32 nm, the positions of the BSW and WGM do not overlap, and the BSW resonance makes the greatest contribution to the mBSW excitation. The most effective excitation of the mBSW occurs when the BSW and WGM resonance positions overlap (bottom layer thickness equals 24 nm). In this case, the dip in reflectance at the mBSW resonance is 5-times greater than both minima of the reflectance relative to the BSW and the WGM.

The appearance of the mBSW is enabled as a result of the effect of the Faraday rotation in the Bi:YIG layers. In the considered MPC with no applied magnetic field ($g=0$), the BSW is excited only for s-polarized light. When a magnetic field is applied to the Bi:YIG layers ($g=0.03$), the light polarization changes due to the Faraday rotation as light passes through the magnetic layers. The presence of the s-polarized component of the field inside the structure leads to the excitation of the mBSW. Because the mBSW is characterized by high field localization at the surface of the MPC and long life time, the effective length of the MPC magnetic layers and corresponding Faraday rotation angle increase.

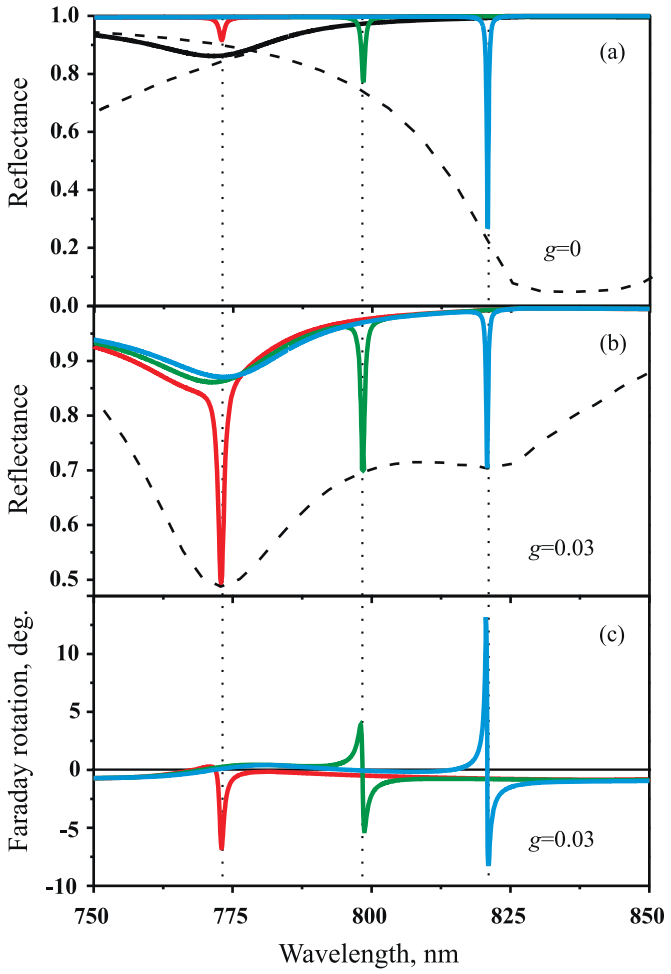

Fig. 5. Spectra of reflectance and Faraday rotation angle of the MPC containing 8 bilayers with different bottom layer thicknesses. Panel (a): magnetic field is absent. Panel (b) and panel (c): magnetic field is present, $g=0.03$ for Bi:YIG layers, p-polarized incident light. Red lines — the thickness of the bottom layer is 24 nm; green lines and black line — the thickness of the bottom layer is 28 nm; blue lines — the thickness of the bottom layer is 32 nm. Dashed lines correspond to reflectance of light at the BSW or WGM (panel (a)) and mBSW (panel (b)) resonance as a function of wavelength, which are shown in Fig. 3. (For interpretation of the references to colour in this figure caption, the reader is referred to the web version of this paper.)

Besides, the effect of the Faraday rotation enhancement can be described with respect to the general properties of the WGM and BSW resonances. The phase of the reflected light varies as a function of light wavelength in the vicinity of any resonance; moreover, the phase change is slow near the resonance with a low Q-factor and exhibits a sharp jump near the resonance with a high Q-factor. The difference in the phase changes in s- and p-polarized light leads to the polarization rotation of the resultant reflected wave and causes the enhancement and change in sign of the Faraday rotation. A similar mechanism for Faraday rotation with changing sign was described for the surface plasmon resonance in magnetoplasmonic structures [11,31].

Thus, the Faraday rotation angle significantly increases and becomes 12° at the wavelength of the mBSW resonance, as shown in Fig. 5. Enhanced Faraday rotation is obtained with a total magnetic layer thickness of only 660 nm and a sample thickness of 1.86 μm. We believe that these unique properties are the result of the mBSW excitation in the structure. The enhancement of the Faraday rotation leads to greater transfer of light energy to the mBSW; therefore, Faraday rotation and mBSW resonance mutually

enhance each other. Thus, the excitation and propagation of Bloch surface waves in an MPC can be efficiently controlled by magnetic field application.

4. Conclusions

In conclusion, the magneto-optical switching of mBSW in a one-dimensional MPC is numerically studied. Analysis of mBSW excitations reveals their dependence on the spectral positions of BSW and WGM resonances. It is shown that the magneto-optical switching of mBSWs appears due to the effect of Faraday rotation and that these effects mutually enhance each other. The maximal value of the Faraday rotation angle is 12°, which is approximately 2 orders of magnitude larger than the value for Bi:YIG thin films with the same total thickness and magneto-optical activity without nanostructuring. The excitation of the mBSW at the surface of the MPC is controlled by the external magnetic field, which presents new opportunities for the design of tunable local microsensors for biological, biochemical and chemical testing.

Acknowledgement

The work was supported by the Russian Science Foundation (#15-02-00065).

References

[1] P. Yeh, A. Yariv, A.Y. Cho, Optical surface waves in periodic layered media, Appl. Phys. Lett. 32 (1978) 104–105, http://dx.doi.org/10.1063/1.89953.
[2] W.M. Robertson, M.S. May, Surface electromagnetic wave excitation on one-dimensional photonic band-gap arrays, Appl. Phys. Lett. 74 (1999) 1800–1802, http://dx.doi.org/10.1063/1.123090.
[3] E. Descrovi, F. Frascella, B. Sciacca, F. Geobaldo, L. Dominici, F. Michelotti, Coupling of surface waves in highly defined one-dimensional porous silicon photonic crystals for gas sensing applications, Appl. Phys. Lett. 91 (2007) 241109, http://dx.doi.org/10.1063/1.2824387.
[4] A. Farmer, A.C. Friedli, S.M. Wright, W.M. Robertson, Biosensing using surface electromagnetic waves in photonic band gap multilayers, Sens. Actuators B 173 (2012) 79–84, http://dx.doi.org/10.1016/j.snb.2012.06.015.
[5] A. Sinibaldi, N. Danz, E. Descrovi, P. Munzert, U. Schulz, F. Sonntag, L. Dominici, F. Michelotti, Direct comparison of the performance of Bloch surface wave and surface plasmon polariton sensors, Sens. Actuators B 174 (2012) 292–298, http://dx.doi.org/10.1016/j.Snb.2012.07.015.
[6] I.V. Soboleva, E. Descrovi, C. Summonte, A.A. Fedyanin, F. Giorgis, Fluorescence emission enhanced by surface electromagnetic waves on one-dimensional photonic crystals, Appl. Phys. Lett. 94 (2009) 231122, http://dx.doi.org/10.1063/1.3148671.
[7] L. Yu, E. Barakat, T. Sfez, L. Hvozdara, J.D. Francesco, H.P. Herzig, Manipulating Bloch surface waves in 2D: a platform concept-based flat lens, Light: Sci. Appl. 3 (2014) e124, http://dx.doi.org/10.1038/lsa.2014.5.
[8] E. Descrovi, T. Sfez, M. Quaglio, D. Brunazzo, L. Dominici, F. Michelotti, H. P. Herzig, O.J.F. Martin, F. Giorgis, Guided Bloch surface waves on ultrathin polymeric ridges, Nano Lett. 10 (2010) 2087–2091, http://dx.doi.org/10.1021/nl100481q.
[9] T. Sfez, E. Descrovi, L. Yu, M. Quaglio, L. Dominici, W. Nakagawa, F. Michelotti, F. Giorgis, H.P. Herzig, Two-dimensional optics on silicon nitride multilayer: refraction of Bloch surface waves, Appl. Phys. Lett. 96 (2010) 151101, http://dx.doi.org/10.1063/1.3385729.
[10] M. Inoue, R. Fujikawa, A. Baryshev, A. Khanikaev, P.B. Lim, H. Uchida, O. Aktsipetrov, A. Fedyanin, T. Murzina, A. Granovsky, Magnetophotonic crystals, J. Phys. D 39 (2006) R151–R161, http://dx.doi.org/10.1088/0022-3727/39/8/R01.
[11] M. Inoue, M. Levy, A.V. Baryshev, Magnetophotonics: From Theory to Applications, Springer Series in Materials Science, 2013.
[12] A.B. Khanikaev, A.V. Baryshev, M. Inoue, Y.S. Kivshar, One-way electromagnetic Tamm states in magnetophotonic structures, Appl. Phys. Lett. 95 (2009) 011101, http://dx.doi.org/10.1063/1.3167356.
[13] A.A. Fedyanin, O.A. Aktsipetrov, D. Kobayashi, K. Nishimura, H. Uchida, M. Inoue, Enhanced Faraday and nonlinear magneto-optical Kerr effects in magnetophotonic crystals, J. Magn. Magn. Mater. 282 (2004) 256–259, http://dx.doi.org/10.1016/j.jmmm.2004.04.058.
[14] A.G. Zhdanov, A.A. Fedyanin, O.A. Aktsipetrov, D. Kobayashi, H. Uchida, M. Inoue, Enhancement of Faraday rotation at photonic-band-gap edge in garnet-based magnetophotonic crystals, J. Magn. Magn. Mater. 300 (2006) 253–256, http://dx.doi.org/10.1016/j.jmmm.2005.10.093.
[15] A.B. Khanikaev, A.B. Baryshev, P.B. Lim, H. Uchida, M. Inoue, A.G. Zhdanov, A. A. Fedyanin, A.I. Maydykovskiy, O.A. Aktsipetrov, Nonlinear Verdet law in magnetophotonic crystals: interrelation between Faraday and Borrmann effects, Phys. Rev. B 78 (2008) 193102, http://dx.doi.org/10.1103/PhysRevB.78.193102.
[16] M. Inoue, K. Arai, T. Fujii, M. Abe, Magneto-optical properties of one-dimensional photonic crystals composed of magnetic and dielectric layers, J. Appl. Phys. 83 (1998) 6768–6770, http://dx.doi.org/10.1063/1.367789.
[17] M. Inoue, K. Arai, T. Fujii, M. Abe, One-dimensional magnetophotonic crystals, J. Appl. Phys. 85 (1999) 5768–5770, http://dx.doi.org/10.1063/1.370120.
[18] T. Goto, A.V. Baryshev, K. Tobinaga, M. Inoue, Faraday rotation of a magnetophotonic crystal with the dual-cavity structure, J. Appl. Phys. 107 (2010) 09A946, http://dx.doi.org/10.1063/1.3365431.
[19] A.A. Fedyanin, T. Yoshida, K. Nishimura, G. Marowsky, M. Inoue, O. A. Aktsipetrov, Nonlinear magneto-optical Kerr effect in gyrotropic photonic band gap structures: magneto-photonic microcavities, J. Magn. Magn. Mater. 258 (2003) 96–98, http://dx.doi.org/10.1016/S0304-8853(02)01072-7.
[20] T.V. Murzina, R.V. Kapra, T.V. Dolgova, A.A. Fedyanin, O.A. Aktsipetrov, K. Nishimura, H. Uchida, M. Inoue, Magnetization-induced second-harmonic generation in magnetophotonic crystals, Phys. Rev. B 70 (2004) 012407, http://dx.doi.org/10.1103/PhysRevB.70.012407.
[21] T. Goto, A.V. Baryshev, M. Inoue, A.V. Dorofeenko, A.M. Merzlikin, A. P. Vinogradov, A.A. Lisyansky, A.B. Granovsky, Tailoring surfaces of one-dimensional magnetophotonic crystals: optical Tamm state and Faraday rotation, Phys. Rev. B 79 (2009) 125103, http://dx.doi.org/10.1103/PhysRevB.79.125103.
[22] T. Goto, A.V. Dorofeenko, A.M. Merzlikin, A.V. Baryshev, A.P. Vinogradov, M. Inoue, A.A. Lisyansky, A.B. Granovsky, Optical Tamm states in one-dimensional magnetophotonic structures, Phys. Rev. Lett. 101 (2008) 113902, http://dx.doi.org/10.1103/PhysRevLett.101.113902.
[23] A.M. Merzlikin, A.P. Vinogradov, A.V. Dorofeenko, M. Inoue, M. Levy, A. B. Granovsky, Controllable Tamm states in magnetophotonic crystal, Phys. B: Condens. Matter 394 (2007) 277–280, http://dx.doi.org/10.1016/j.physb.2006.12.027.
[24] G. Lu, J. Da, Q. Mo, P. Chen, Manipulating optical Tamm state in one dimensional magnetophotonic crystal by anisotropic materials, Physica B 406 (2011) 4159–4162, http://dx.doi.org/10.1016/j.physb.2011.08.031.
[25] D.W. Berreman, Optics in stratified and anisotropic media: 4×4-matrix formulation, J. Opt. Soc. Am. 62 (1972) 502–510, http://dx.doi.org/10.1364/JOSA.62.000502.
[26] D.S. Bethune, Optical harmonic generation and mixing in multilayer media: extension of optical transfer matrix approach to include anisotropic materials, J. Opt. Soc. Am. B 8 (1991) 367–373, http://dx.doi.org/10.1364/JOSAB.8.000367.
[27] H. Kato, T. Matsushita, A. Takayama, M. Egawa, K. Nishimura, M. Inoue, Theoretical analysis of optical and magneto-optical properties of one-dimensional magnetophotonic crystals, J. Appl. Phys. 93 (2003) 3906–3911, http://dx.doi.org/10.1063/1.1559422.
[28] M. Vasiliev, V.I. Belotelov, A.N. Kalish, V.A. Kotov, A.K. Zvezdin, K. Alameh, Effect of oblique light incidence on magnetooptical properties of one-dimensional photonic crystals, IEEE Trans. Magn. 42 (2006) 382–388, http://dx.doi.org/10.1109/TMAG.2005.862765.
[29] I.H. Malitson, Interspecimen comparison of the refractive index of fused silica, Opt. Soc. Am. 55 (1965) 1205–1209, http://dx.doi.org/10.1364/JOSA.55.001205.
[30] S. Wittekoek, Th.J.A. Popma, M.J. Robertson, P.F. Bongers, Magneto-optic spectra and the dielectric tensor elements of bismuth-substituted iron garnets at photon energies between 2.2–5.2 eV, Phys. Rev. B 12 (1975) 2777–2788, http://dx.doi.org/10.1103/PhysRevB.12.2777.
[31] A.B. Khanikaev, A.V. Baryshev, A.A. Fedyanin, A.B. Granovsky, M. Inoue, Anomalous Faraday effect of a system with extraordinary optical transmittance, Opt. Express 15 (2007) 6612–6622, http://dx.doi.org/10.1364/OE.15.006612.